# Surface Tension Measurements by Means of the "Microcone Tensiometer"

WILFRIED HELLER, MIEN-HSIUNG CHENG, AND BETTYE W. GREENE<sup>2</sup>

Department of Chemistry, Wayne State University, Detroit, Michigan 48202

Received September 20, 1965

#### INTRODUCTION

An observation undoubtedly made by virtually every experimental chemist is the following: if, after emptying a pipet, a drop remains halfway inside the conical end section, this drop will move to the narrow tip no matter whether the tip is pointing downward (case 1) or is horizontal (case 2). If it is pointing upward, the drop will move to a wider section of the conical end until it assumes an equilibrium position (case 3). In the most striking case 2, the movement is due exclusively to the difference in surface pressure at the two ends of the conical drop. In case 1 this pressure difference cooperates with the pressure resulting from gravity; in case 3—the only one where an equilibrium position of the drop inside the pipet is possible with well wetting liquids—the position of the drop is dictated by the competition between excess surface pressure and gravitational pressure. It is clear that this last phenomenon can be used for determining surface tensions of liquids or solutions using as little as 10<sup>-4</sup> ml. The detailed theory of this almost completely ignored phenomenon has been developed recently (1). The present paper is concerned with its practical application. There exists no literature on pertinent experimentation.

- <sup>1</sup> This work was supported in part by a grant from the National Institute of Health.
- <sup>2</sup> During the early experimental phase of this project, Dr. N. Tanaka contributed to it with a series of helpful semiquantitative measurements not considered here.

### I. BRIEF REVIEW OF THE THEORY

Figure 1 gives a schematic picture of a conical capillary (fully drawn quadrangle) the axis of which forms an angle,  $\omega$ , with the vertical. It contains a drop, of axial length H, of a liquid which has a contact angle  $\beta < 90^{\circ}$ . The drop assumes an equilibrium position, defined by  $h_1$  and  $h_2$ , in that section of the capillary where the pressure exerted by the weight of the drop upon the larger liquid-air surface  $S_2$ 

$$P_H = V_e \, \Delta \rho g \, \cos \, \omega / S_2 \tag{1}$$

is just balanced by the excess surface pressure acting upon the smaller liquid-air surface  $S_1$ 

$$P_S = 2\pi\gamma \{ [R_1 \cos(\beta - \alpha)/S_1] - [R_2 \cos(\beta + \alpha)/S_2] \}.$$
 [2]

Here,  $V_e$  is the effective volume of the drop,  $\Delta_{\rho}$  is the density difference between the drop and the surrounding gas phase,  $R_1$  and  $R_2$  are the capillary radii at the level of the respective liquid-glass-air junctions, g is the gravitational constant, and  $\alpha$  defines the cone to the extent needed here. From the preceding equations, one obtains at once the surface tension

$$\gamma = \frac{V_e \, \Delta \rho g \, \cos \, \omega / 2\pi S_2}{[R_1 \cos \, (\beta - \alpha) / S_1] - [R_2 \cos \, (\beta + \alpha) / S_2]}$$
[3]

if  $\beta < 90^{\circ}$  and

$$\gamma = \frac{V_e \, \Delta \rho g \, \cos \omega / 2\pi S_1}{[R_2 \cos (\beta + \alpha) / S_2] - [R_1 \cos (\beta - \alpha) / S_1]}$$
[4]

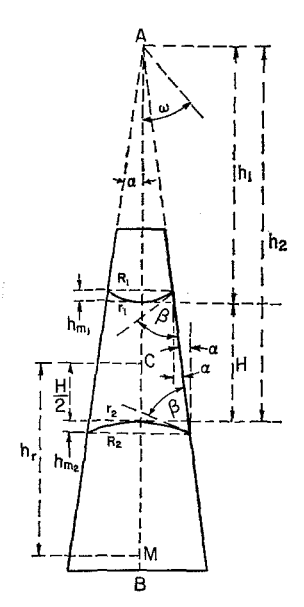


Fig. 1. Schematic illustration of method and of quantities contained in equations

if  $\beta > 90^{\circ}$ , it being necessary, in the latter case, that the tip of the cone faces downward ( $\omega > 90^{\circ}$ ).

In order to arrive at a practically convenient expression,  $V_e$  has to be replaced by easily measurable quantities. Furthermore, both menisci have to be taken into account. The latter is done assuming the menisci to represent segments on a spherical surface. This assumption is valid in sufficiently narrow capillaries. One thus obtains, eventually, for  $\beta < 90^{\circ}$ , the explicit exact expression

$$\gamma = A\Delta\rho g \cos\omega/B, \qquad [5]$$

where

$$A = R_2^2 (H + h_{m_2} + h_{m_1}) - \frac{1}{3} (h_{m_1}^3 G_1 + h_{m_2}^3 G_2)$$
 [6]

and

$$B = 2(R_2/R_1)[R_2\cos(\beta - \alpha) - R_1\cos(\beta + \alpha)].$$
 [7]

Here.

$$h_{m_1} = R_1 \tan \xi_1;$$
 [8]

$$h_{m_2} = R_2 \tan \xi_2$$
; [8a]

$$G_1 = (2 + \cos 2\xi_1)/(1 - \cos 2\xi_1);$$
 [9]

$$G_2 = (2 + \cos 2\xi_2)/(1 - \cos 2\xi_2); [9a]$$

where

$$\xi_1 = \frac{\pi}{4} - \frac{1}{2} (\beta - \alpha);$$
 [10]

$$\xi_2 = \frac{\pi}{4} - \frac{1}{2} (\beta + \alpha).$$
 [10a]

If  $(\alpha + \beta) < 3^{\circ}$ , one will, as explained elsewhere (1), commit only a small error in  $\gamma$  on replacing A in Eq. [6] by

$$A' = H + \frac{1}{3}R_2 + R_1(1 - \frac{2}{3}R_1^2/R_2^2)$$
 [6a]

and B in Eq. [7] by

$$B' = 2\{ [\cos(\beta - \alpha)/R_1] - [\cos(\beta + \alpha)/R_2] \}.$$
 [7a]

If, in addition,  $\beta = 0^{\circ}$  (aqueous solutions) B' simplifies to

$$B'' = 2 \cos \alpha \left( \frac{1}{R_1} - \frac{1}{R_2} \right).$$
 [7b]

Finally, if  $(\alpha + \beta) \ll 3^{\circ}$  and  $H \ge 1$  cm., and if no more than three significant figures are needed for  $\gamma$ , one may simplify Eq. [6a] further to

$$A'' = H + \frac{1}{3}(R_1 + R_2).$$
 [6b]

In the case of well wetting liquids, including  $H_2O$  and aqueous solutions,  $(\alpha + \beta)$  will always be far smaller than required by the simpler equations since  $\beta$  is then always small or zero and since, in addition,  $\alpha$  must necessarily be kept very small if the capillaries are to have a convenient length. (Consider, for instance, a capillary as short as 20 cm. with the two terminal inner radii of 0.05 and 0.15 mm.,  $\alpha < 0^{\circ}2'$ .) It will therefore, in general, be possible, to operate with the simple equations [5], [6a], and [7a]and, in the case of aqueous solutions, with Eqs. [5], [6a], and [7b]. The comparative performance of the various equations will be tested later on a few examples.

#### II. THE APPARATUS

Figure 2 shows the "microcone tensiometer." The capillary is inserted in a conventional reflux condenser and is held in place by means of two perforated corks or rubber stoppers  $D_1$  and  $D_2$ . The purpose of the

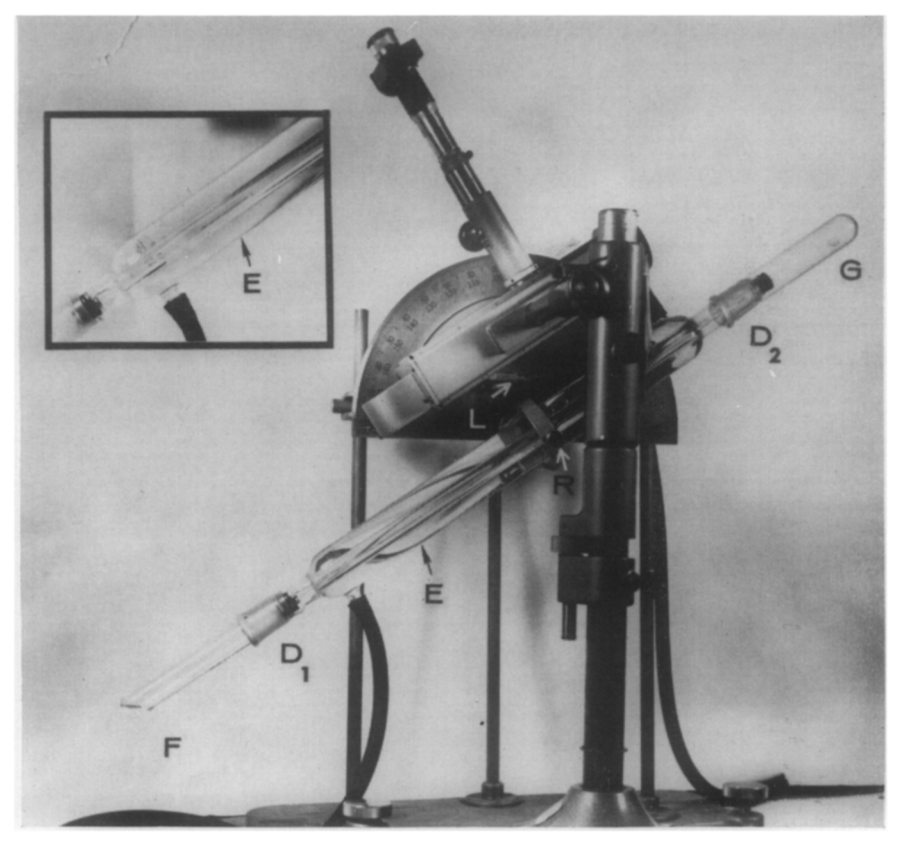


Fig. 2. The apparatus

reflux condenser is to thermostat the capillary, water from a thermostat being pumped through it continuously. The liquid drop, of nearly cylindrical shape, inside the capillary is seen at E. This section of the apparatus is shown, in magnified reproduction, in the rectangular inset. The position of the drop in the capillary can be changed at will by changing the inclination of the capillary with respect to the vertical (the angle  $\omega$ ). To that effect, the reflux condenser and, with it, the capillary can be rotated about a horizontal axis at R. If solutions in common solvents are investigated, a small amount of solvent is placed in F in order to speed up equilibration between the drop and the surrounding gas phase. In Fig. 2 it is assumed that  $\beta < 90$ . If  $\beta > 90$ , the condenser would have to be turned so that the narrow end of the capillary, facing G, faces downward. A large protractor to which a level, L, is attached gives a preliminary, rough value of  $\omega$ . Next to the apparatus is the traveling microscope needed for the measurements of H and of the quantity  $h_{\tau}$  (see Section III). It is provided with a filar eyepiece micrometer, a special attachment, which is needed for exact  $\omega$  determinations (see Section V).

# III. CALIBRATION OF THE CAPILLARY FOR ABSOLUTE $_{\gamma}$ DETERMINATIONS WITHOUT USE OF AN INSTRUMENT CONSTANT

The calibration of the conical capillary has to be carried out with great care if the method is to yield absolute surface tension data of high accuracy. The calibration experiments are, in principle, identical with those needed with cylindrical capillaries (such as used in connection with the capillary height method). They differ, in detail, from the latter in two respects: (a) several sets of calibration data are necessary instead of the single set which suffices with cylinders; (b) the treatment of the calibration data is somewhat more time consuming.

Working with a carefully cleaned capillary and triple distilled Hg, the axial length H of a drop of Hg of exactly known weight is determined with a traveling microscope for systematically varied values of  $h_r$ . The latter quantity is, as shown in Fig. 1,3 the distance from an arbitrary reference mark, M, engraved near the wide end of the capillary, to the center, C, of the conical drop of Hg in the capillary. (In actual work, several auxiliary reference marks, spaced at about equal intervals between M and the tip, were used for the sake of convenience. At least two such marks can be detected easily in the inset to Fig. 2.) Not only the variation of the capillary radius, r, with  $h_r$  but also  $\alpha$  and its possible variation with  $h_r$  are a priori unknown. An immediate direct determination of both quantities by a single series of calibrations is not possible. It is therefore necessary that the mean radius  $\bar{r}$  be calculated first, at any  $h_i$ , by considering the Hg drop of volume,  $V_{\rm Hg}$ , in a first approximation as a cylinder which contains a hemispheric meniscus at each end, viz.,

<sup>3</sup> In the present instance, the menisci have, of course, a curvature opposite to that given in Fig. 1.

$$V_{\rm Hg} = \bar{r}^2 \pi H - \frac{2}{3} \bar{r}^3 \pi.$$
 [11]

(Since  $\beta > 90^{\circ}$ , H is here the distance between the summits of the two menisci in contradistinction to the situation illustrated by Fig. 1.) For the sake of convenience, one will, in general, prefer not to calculate  $\bar{r}$  from Eq. [11], but rather in two steps, first by evaluating the quantity  $\bar{r}_0^2$  which neglects the menisci

$$\bar{r}_0^2 = \frac{V_{\rm Hg}}{\pi H} \tag{12}$$

and subsequently by calculating  $\tilde{r}^2$  itself from

$$\bar{r}^2 = \bar{r}_0^2 \left( 1 + \frac{2\bar{r}_0^3 \pi}{3V_{\text{Hg}}} \right) = \bar{r}_0^2 \left( 1 + \frac{2\bar{r}_0}{\pi H} \right).$$
 [13]

(The correction factor in Eq. [13] clearly will be consequential only at small H.)

The  $\bar{r}$  values thus obtained as a function of  $h_{\tau}$  give a calibration curve which is sufficient if used in connection with an instrument constant (Section IV). If absolute  $\gamma$  measurements are to be made, the calibration just described must be repeated with systematically varied Hg volumes in order to find the true radius, r, and its variation

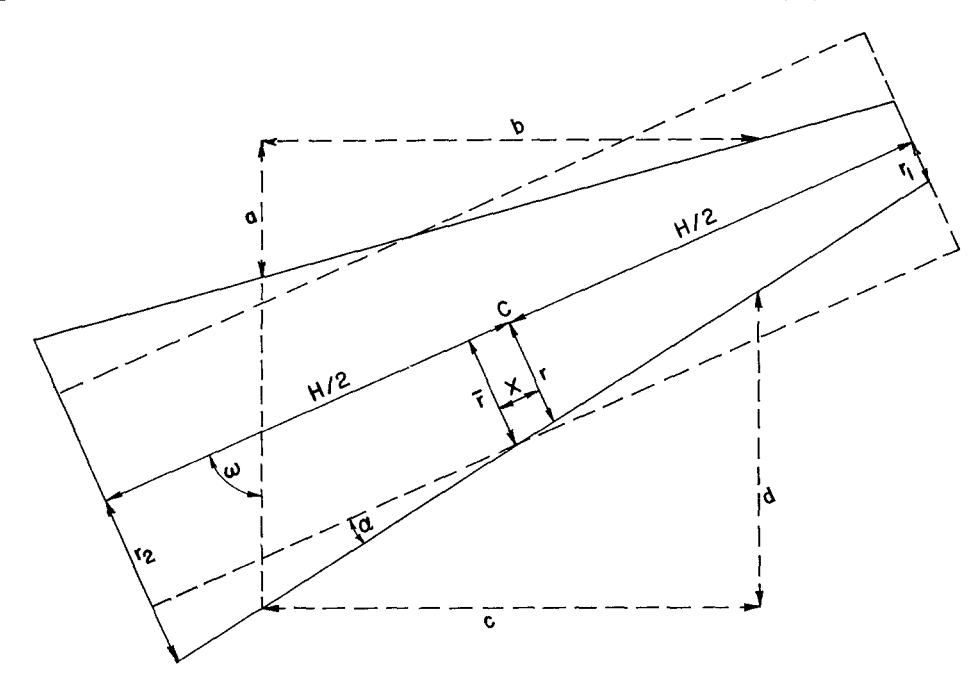


Fig. 3. Illustration and definition of some quantities used in Eqs. [14]-[19], [23], and [27]

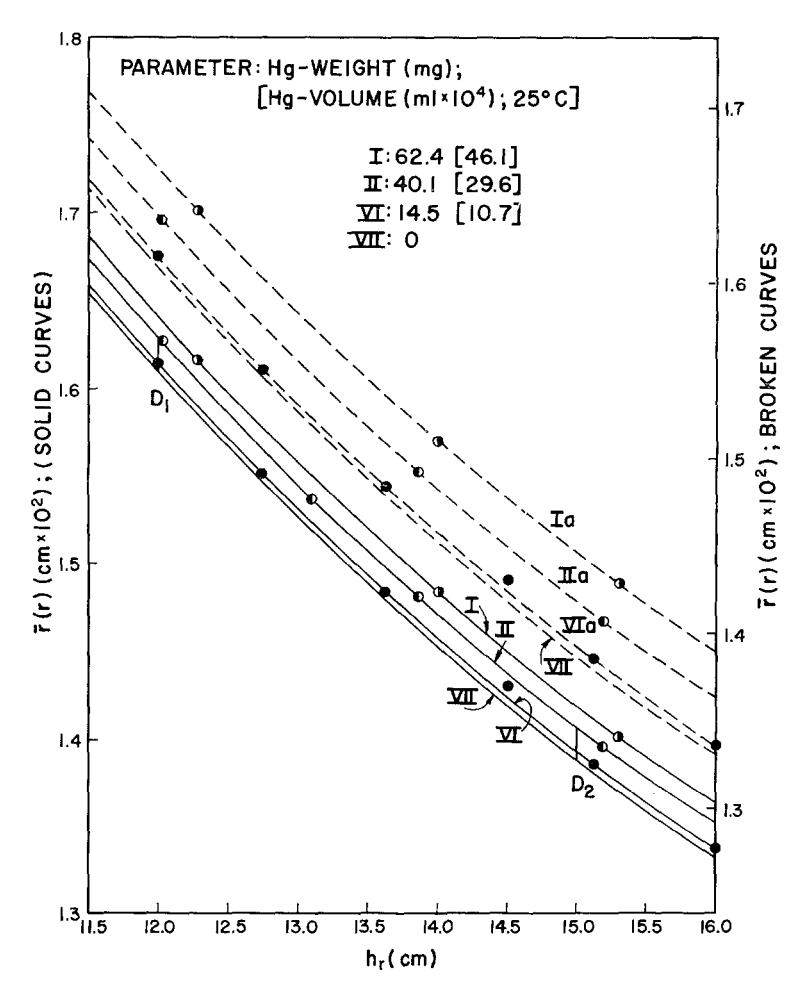


Fig. 4. Detailed calibration curves for a limited section of the conical capillary used. For details see text.

with  $h_i$ . The procedure to be followed may be explained by means of schematic Fig. 3. It is clear that the true radius, r, at C (i.e., at the distance  $h_r$  from M) is smaller than  $\bar{r}$ . In view of the simple relations

$$r_1 = r - \frac{H}{2} \tan \alpha \qquad [14]$$

and

$$r_2 = r + \frac{H}{2} \tan \alpha, \qquad [15]$$

and since

$$\bar{r}^2 = \frac{1}{3}(r_1^2 + r_1r_2 + r_2^2),$$
 [16]

the relation between  $\tilde{r}(H)$  and r follows as

$$\bar{r}^2 = r^2 + \frac{H^2 \tan^2 \alpha}{12}.$$
 [17]

Furthermore, in view of

$$r = \frac{r_1 + r_2}{2}, \qquad [18]$$

the error in the  $h_{\tau}$  value

$$x = H^2 \tan \alpha / 12(r_1 + r_2).$$
 [19]

Equation [17] allows one to obtain the true r vs.  $h_r$  curve if several  $\bar{r}$  vs. h, calibration curves, obtained with systematically varied  $V_{\rm Hg}$ , are available. One simply constructs, for systematically varied  $h_r$  values as parameter,  $\bar{r}^2$  vs.  $H^2$  plots (or equivalent other plots). The intercept of such plots yields the true  $r^2$  for a given  $h_r$ . The variation of r with  $h_r$  thus obtained, by extrapolation, is shown, for a limited section of

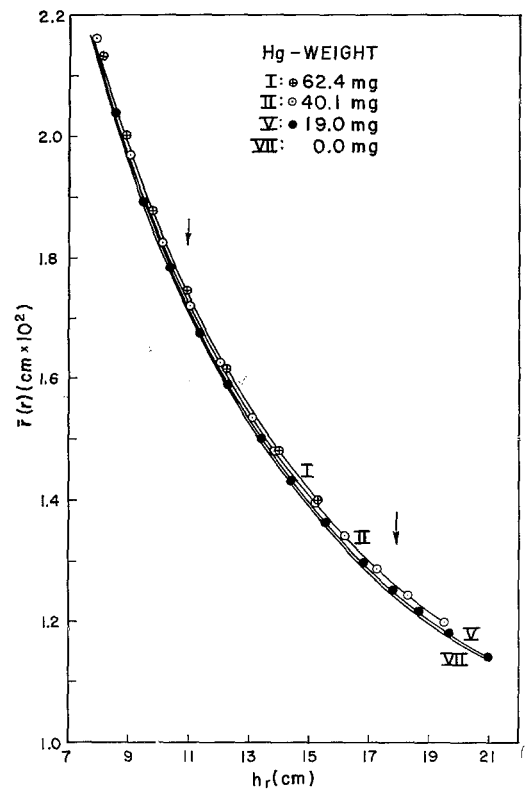


Fig. 5. Calibration curves for entire practically useful length of conical capillary. (For meaning of two arrows, see Section VII, 1.)

the capillary, by curve VII in Fig. 4. Curves I, II, and VI are  $\bar{r}$  vs.  $h_r$  curves, the weight (W) or volume of Hg used for the calibration at 25°C,  $(V_{\rm Hg}^{25})$  being the parameter. Three important additional  $\bar{r}$  vs.  $h_r$  curves, for  $\bar{V}_{\rm Hg}^{25}=19.0\times10^{-4},17.6\times10^{-4},$  and  $14.0\times10^{-4}$  ml., are not shown in order not to overload the figures. (The curves Ia, IIa, and VIa will be discussed later.) Three of the experimental curves and the extrapolated curve are shown in Fig. 5 for the entire most useful section of the same capillary. (Radii larger than 0.20–0.22 and smaller than 0.10–0.12 mm. are practically less useful than intermediate radii.)

It is important to describe in more detail the methods available for obtaining, by extrapolation, the true r vs. h, curve. The  $\bar{r}^2$  vs.  $H^2$  plots already referred to should represent straight lines for any H range if  $\alpha$  is constant. This was not the case with the homemade capillaries used in the

present work. Here,  $\alpha$  varied with  $h_r$  (see Fig. 8) and, consequently, the mean  $\bar{\alpha}$ , at a given  $h_r$ , varied with H. Therefore, the  $\bar{r}^2$  vs.  $H^2$  plots are, in reality, straight lines only as long as H is small enough so that the variation of  $\alpha$  between  $R_2$  and  $R_1$  can be disregarded. With capillaries of the type used in this work,  $\bar{r}^2$  vs.  $H^2$  plots have therefore no advantage over practically more convenient  $\bar{r}$  vs.  $H^2$  plots. These alternate plots used primarily in the present work give r directly as the intercept. The pertinent equation, which follows from Eq. [17] by expansion, is

$$\bar{r} = r + \frac{H^2 \tan^2 \alpha}{24r} - \frac{H^4 \tan^4 \alpha}{1152r^3} + \cdots$$
 [20]

The limiting slope extends over a sufficiently wide range of H values to allow a secure extrapolation to r particularly if the variation of  $\alpha$  between  $R_1$  and  $R_2$  is taken into account. This is apparent from Fig. 6, where the limiting slope is seen to be constant for the four lowest Hg volumes (four lowest H values) used, after the variation of  $\alpha$  with  $h_r$  has been corrected for (full circles). It should be noted that the correction does not alter the two lowest points of the plots. Here corrected and uncorrected (open circles) data coincide.

The open circles represent the primary uncorrected data based upon considering the drop as equivalent to a cylinder of radius  $\bar{r}$  having a volume identical to that of a truncated cone of constant \( \alpha \) (Eq. [16] (Fig. 3)). This simple truncated cone is subsequently replaced by two truncated cones, A and B, of differing  $\alpha$  but equal length, which are contiguous at  $h_r$ . To that effect, a preliminary tracing of  $\alpha$  vs.  $h_r$  is made by means of the  $\bar{r}$  vs.  $h_r$  curve obtained with the smallest Hg volume (curve VI in Fig. 4). (For the final  $\alpha$  vs.  $h_r$  curve see Fig. 8.) With H and  $h_r$  known, the  $\alpha$  values,  $\alpha_2$  pertinent to  $h_r$ ,  $\alpha_1$  pertinent to  $[h_r -$ (H/2)], and  $\alpha_3$ , pertinent to  $[h_r + (H/2)]$ , are available at once. For the calculation of the volume of one of the two cones, the  $\alpha$  value  $\bar{\alpha}_A$  =  $(\alpha_1 + \alpha_2)/2$  is used; for the calculation of the volume of the contiguous cone,  $\alpha_B = (\alpha_2 + \alpha_3)/2$  is used. The corrected  $\bar{r}$  value obtained from such a double cone (full circles) represents therefore the radius of a cylinder having a volume identical with that of a cone of stepwise varied  $\alpha$ . An unnecessary minor further improvement in the  $\bar{r}$  values could be obtained by replacing the

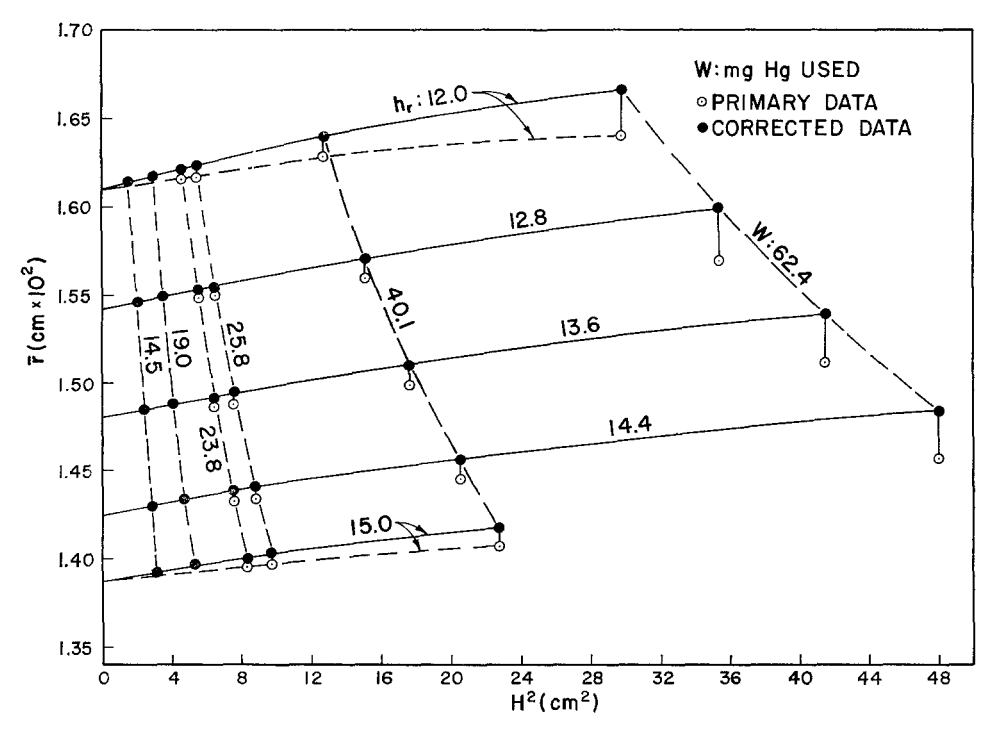


Fig. 6. Graphical evaluation of true capillary radius according to Eq. [20]

truncated cone by 3 or 4 contiguous differential cones of varied  $\alpha$ .

In order to get plots of the type shown in Fig. 6 for  $h_r$ -values which have 3 significant figures. To that effect all points pertinent to a given  $h_r$  were read off a set of large master calibration curves. Sections of some of them were shown in Fig. 4. The lower series of curves (Roman numerals only) are the basis for the uncorrected values (open circles) in Fig. 6. The upper series of curves (Roman numerals followed by the letter a) represent the corrected values (identified by full circles in Fig. 6).

Whereas  $\bar{r}$  vs.  $H^2$  plots as illustrated by Fig. 6 are very satisfactory, they are affected by the slight inconvenience that the location, with respect to the abscissa, of the points pertinent to the same Hg weight, varies with  $h_r$ . This is avoided on using as the independent variable the square of the volume or of the weight, W, of Hg. The slope of the  $\bar{r}^2$  vs.  $W^2$  plots is according to Eq. [17]

$$\tan^2\alpha/12 \ \bar{r}^4\pi^2\rho_{\rm Hg}^2$$

and the limiting slope of  $\bar{r}$  vs.  $W^2$  plots is, according to Eq. [20],

$$\tan^2\alpha/24 r\bar{r}^4\pi^2\rho_{\rm Hg}^2$$
,

where  $\rho_{\text{Hg}}$  is the density of Hg. At low and moderate W values, a practically straight line is obtained, allowing again a simple extrapolation to r. Examples of such plots are given in Fig. 7.

Having established the r vs.  $h_r$  calibration curve, the angle  $\alpha$  and its variation with  $h_r$  must be determined. One may use the slope of either  $\bar{r}^2$  vs.  $H^2$  or  $\bar{r}$  vs.  $H^2$  plots for the evaluation of  $\alpha$  and of its variation with  $h_r$ . However, it was found simpler to obtain this information from a chord plot derived from the r vs.  $h_r$  curve (curve VII in Fig. 5). The resulting tan  $\alpha$  vs.  $h_r$  curve is given in Fig. 8.4 The latter data, in conjunction with the r vs.  $h_r$  data discussed above, form the basis for absolute  $\gamma$  determinations with the present method, as described in Section VII.

# IV. CALIBRATION OF THE CAPILLARY FOR $\gamma$ DETERMINATIONS USING AN INSTRUMENT CONSTANT

If it is not necessary to achieve the highest possible accuracy for  $\gamma$  and, particularly, if it is sufficient to *convert* measured data

<sup>4</sup> The bars of length  $\Delta h_r$  represent the mean  $\tan \alpha$  between the limits of  $h_r$  indicated.

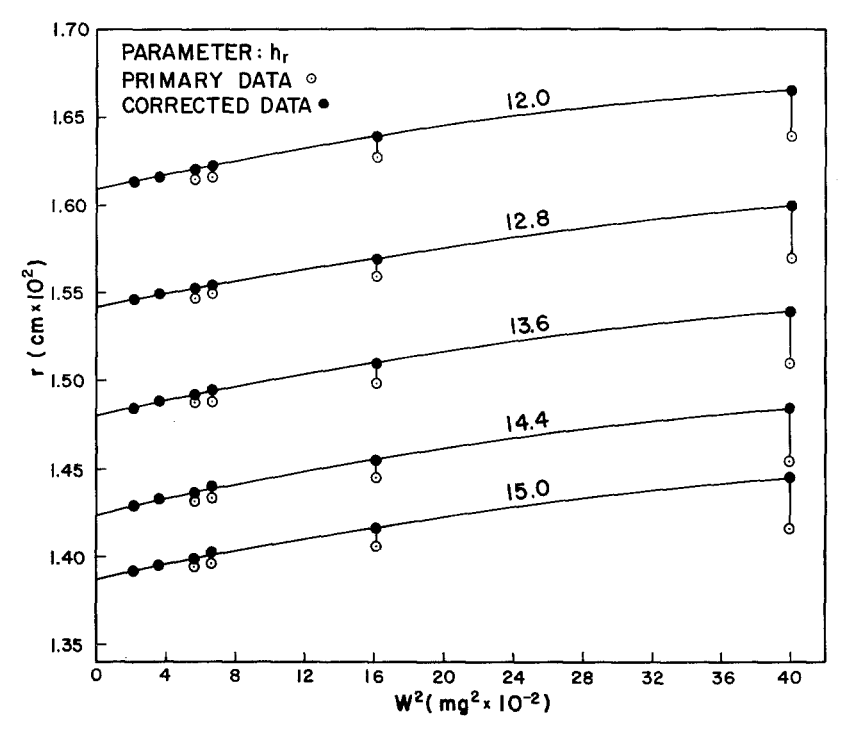


Fig. 7. Alternate graphical evaluation of true capillary radius

into absolute  $\gamma$  values by means of an "instrument constant," then the capillary calibrations may be simplified appreciably. It will then suffice to compile just one calibration curve, for instance, curve II in Fig. 4 (5). One may bring this curve into coincidence with the extrapolated curve, VII, by means of a factor  $D = f(h_r)$ . Fortunately, the variation of D with  $h_r$  is only slight particularly at large  $h_r$ -(small  $\alpha$ )-values. Thus the specific factors  $D_1$  and  $D_2$  at  $h_r =$ 12 and 15 cm., respectively, indicated in Fig. 4 differ by only 5-6%. Therefore, a single conversion factor  $\bar{D}$  will be justified as long as  $h_r$  is not varied within wide limits. Whenever a single  $\bar{D}$  value is applicable, the apparent  $\gamma$  values,  $\gamma_{ap}$ , determined with the aid of a single  $\bar{r}$  vs.  $h_r$  curve (e.g., curve II in Fig. 4) may therefore be corrected by means of a single correction factor (instrument constant) C, provided the variation of C with the pertinent variables does not exceed that of D. In order to check this point the quantitative relationship between C and D had to be determined. For the present purpose, it is sufficient to use the simplest

equations, viz., Eqs. [6b] and [7b], in conjunction with Eq. [5], in order to define this relationship.

Representing  $\gamma/\Delta\rho g$  cos  $\omega$  by F, one has

$$F = \frac{HR_1R_2 + (\frac{1}{3})R_1R_2(R_1 + R_2)}{2\cos\alpha(R_2 - R_1)}.$$
 [21]

On the other hand, the apparent  $F_1$  value,  $F_{ap}$ , derived by means of a single calibration curve, such as curve II in Fig. 4,

$$F_{ap.} = \frac{H\bar{R}_1 \,\bar{R}_2 + (\frac{1}{3})\bar{R}_1 \,\bar{R}_2(\bar{R}_1 + \bar{R}_2)}{2 \cos \alpha(\bar{R}_2 - \bar{R}_1)}. \quad [22]$$

On omitting, as inconsequential, terms containing  $\bar{D}^2$  and  $\bar{D}^3$ , one obtains

$$\frac{F}{F_{ap.}} = \frac{\gamma}{\gamma_{ap.}} = 1$$

$$-\frac{\bar{D}[H(\bar{R}_1 + \bar{R}_2) + (\frac{1}{3})(\bar{R}_1^2 + \bar{R}_2)]}{H\bar{R}_1\bar{R}_2 + (\frac{1}{3})\bar{R}_1^2\bar{R}_2 + (\frac{1}{3})\bar{R}_1\bar{R}_2^2}.$$
[23]

The second term in Eq. [23] evidently represents the explicit value of the correc-

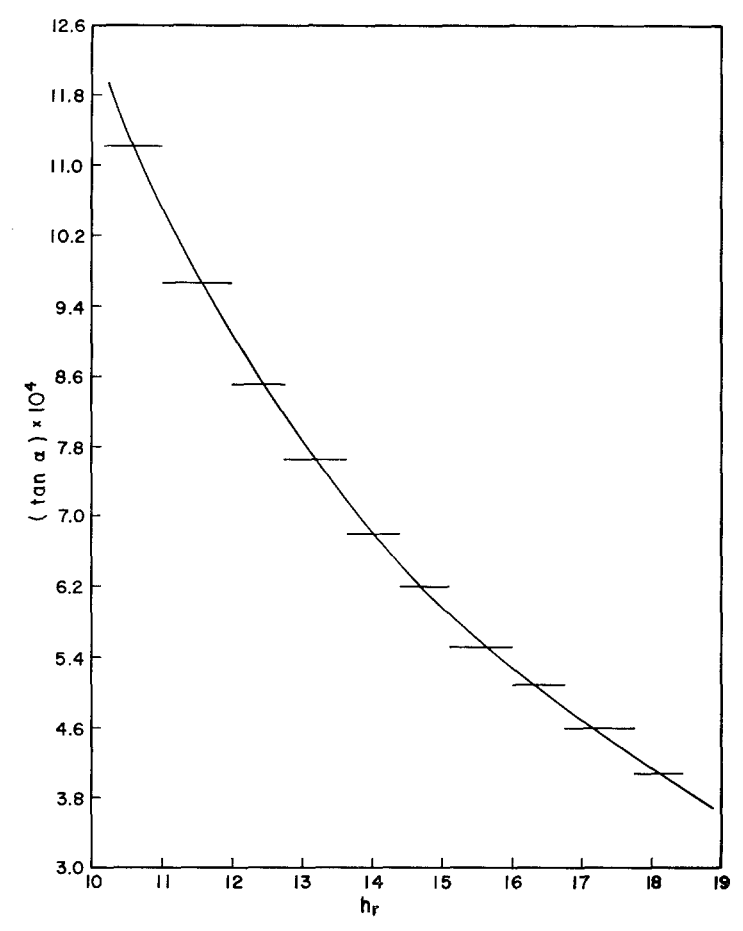


Fig. 8. Graphical determination of the  $(\tan \alpha)$  vs.  $h_r$  function

tion factor (instrument constant) C in Eq. [24]

$$\gamma = \gamma_{ap} (1 - C), \qquad [24]$$

where the "apparent" surface tension  $\gamma_{ap}$  is assumed to have been derived from a single r vs.  $h_r$  calibration curve. If  $R_1 \ll H \gg R_2$ , and  $\alpha < 1^\circ$  (this will generally apply), the second term in Eq. [23] may be simplified to

$$C = \bar{D} \left[ \frac{\bar{R}_1 + \bar{R}_2}{\bar{R}_1 \bar{R}_2} + \frac{2}{H} \right].$$
 [25]

It follows from Eq. [25] that  $(C/\bar{D})$  is not a constant unless  $R_1$  and  $R_2$  are always the same. Within the  $h_r$  range for which one may consider  $\bar{D}$  as a constant, C will, at constant  $h_r$ , increase with H and, at constant H, decrease with  $h_r$ . If the convenience of a single instrument constant is to be

taken advantage of, it is therefore advisable not to vary  $h_r$  within more than modest limits and to use roughly the same liquid volumes. The former condition can fortunately be met easily by adjusting  $\omega$  according to need and the latter condition represents no problem.

The last remaining question pertains to the actual practical procedure to be used in order to find a value of C for a particular section of a capillary. This is done by using a single calibration curve for the calculation of the apparent surface tension  $\gamma_{ap}$ , of a liquid of known surface tension  $\gamma$ . For this purpose, one also has to use the apparent  $\alpha_{ap}$  vs.  $h_r$  curve ( $\alpha_{ap}$ : the apparent  $\alpha$  value). From Eq. [24] C follows at once. From C, in turn,  $\bar{D}$  can be obtained immediately, if desired.

The value of C (and/or  $\bar{D}$ ) having been established for a given section of a capillary (for a given approximate  $h_r$  range), it will be wise to determine the limits existing, beyond the  $h_r$  range selected, for the application of a single C value without risking significant errors in the results. For this purpose, the liquid drop may be shifted systematically in both directions until  $\gamma$ , calculated from Eq. [24], ceases to be a constant on using the single value of C. One may, of course, if desired, establish the variation of C with  $h_r$  and H if the entire length of the capillary is to be used with various liquid volumes.

Actual numerical  $\gamma$  determinations by means of an instrument constant are included and discussed in Section VII.

All the experiments reported below were carried out with a single capillary. Its characteristics were as follows: Overall length: 38 cm.; length of experimentally useful calibrated section: 13.5 cm.; limiting diameters within calibrated section: largest:  $5 \times 10^{-2}$  cm.; smallest:  $2.1 \times 10^{-2}$  cm.; liquid volume needed to give a cylindrical drop of 1 cm. length at narrow end:  $3.83 \times 10^{-4}$  ml.

#### V. DETERMINATION OF ω

The larger  $\omega$ , the more important is its accurate determination. In order to make accurate determinations relatively easy, the traveling microscope is equipped with an eyepiece micrometer (Fig. 2) so that distance measurements in two orthogonal directions are possible. The character of the measurements follows from Fig. 3. Starting to the left of C at the upper wall of the capillary, an arbitrary distance, a, is covered by vertical displacement of the tubus of the traveling microscope. Next, the eyepiece micrometer is displaced horizontally over the distance, b, until the capillary wall is reached again. The measurement of a and b is followed by that of the distances c and dat the lower wall of the capillary. This completes one pair of measurements. The simple relationships to be used for the calculation of  $\omega$  are:

$$a/b = \cot(\omega + \alpha);$$
 [26]

$$c/d = \tan(\omega - \alpha).$$
 [27]

The  $\omega$  value actually used is the mean of the results obtained with Eqs. [26] and [27]. In case of major divergence of the two primary  $\omega$  values, one or more additional pairs of measurement are made.

## VI. EFFECT OF VISCOSITY AND SURFACE ROUGHNESS

A change in  $\omega$  will cause the conical drop in the capillary to move until it assumes a new stationary position. With water and aqueous NaCl solutions, the only systems studied thus far, the kinetics is practically the same. It takes the conical drop close to 25 seconds to cover half the distance between its old and its new stationary position but nearly 10 minutes before the movement stops completely. The asymptotic  $h_r$  vs. time curve is almost the same for movement towards either the wide or the narrow end of the capillary. Although the attainment of a new stationary position is slow, it is important to note that the very small changes found after 3 minutes do not lead to changes of  $\gamma$  outside of the limits of the overall experimental error (see Tables I and II). It also should be noted that the rate at which the menisci approach their final position, increases with the capillary radius. The preliminary numerical data just given apply to a radius < 0.2 mm. The conclusion to be drawn from these observations is that it is advisable to watch the two menisci for a sufficient period of time so as to be sure that they have reached their final or practically final position for the particular  $\omega$  value selected. These phenomena are, of course, completely analogous to those observed on forcing a change in level in the capillary height method. In that method, possible errors due to slow creep are mostly disregarded.

It is important to realize that the final position reached by the conical drop is a true equilibrium position only if the inner surface of the capillary is ideally smooth. If it is not ideally smooth (none of the capillaries tested by us turned out to have an ideally smooth inner surface), the true position of equilibrium between gravitational

<sup>&</sup>lt;sup>5</sup> In contradistinction to  $\gamma$ , the variation of the individual  $\gamma_{i^-}$  values (see Section VII) is not negligible prior to about 10 minutes.

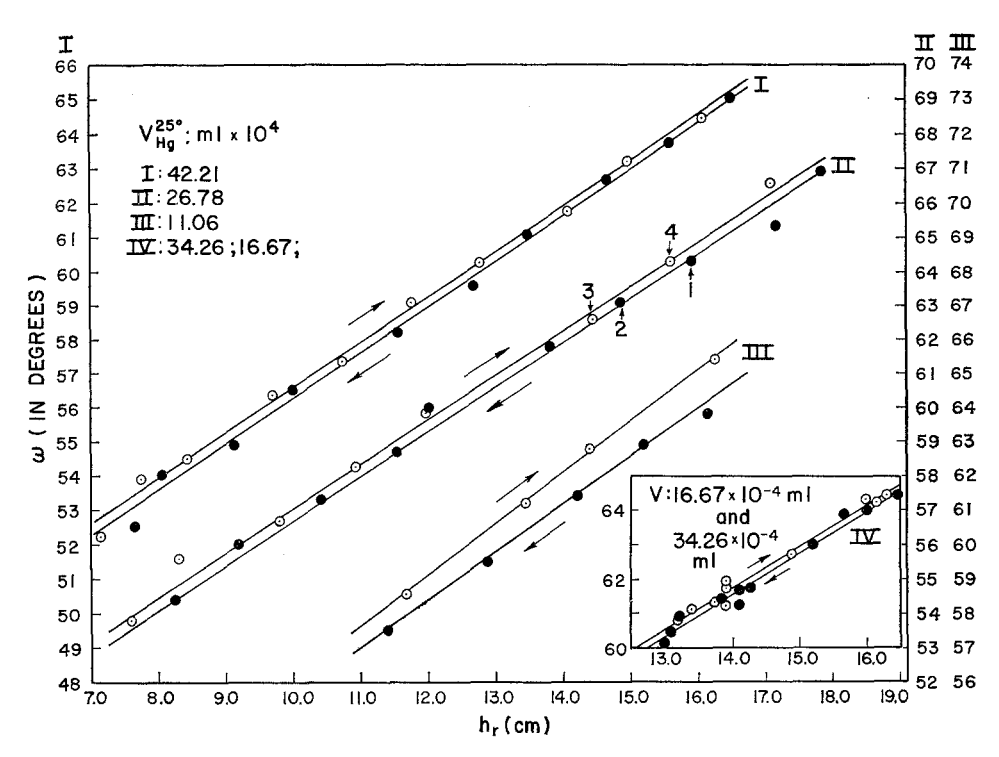


Fig. 9. Dependence of  $h_r$  on  $\omega$  and the direction of flow in the capillary. *Inset:* Data taken from Table I

and excess surface pressure will not be reached but must be found indirectly. The problem and its solution follow readily from Fig. 9. Open circles represent the final  $h_r$ value attained after flow towards the wide end of the capillary subsequent to a reduction in  $\omega$  to the value indicated on the ordinate. Full circles represent the final  $h_r$ value reached after flow, in the opposite direction, subsequent to an increase in  $\omega$  to the value indicated on the ordinate. It is seen that a single curve cannot satisfy both open and full circles even on making allowance for the scattering of the data. Considering, for example,  $\omega = 63^{\circ}$  and the curve pair II, it is seen that on flow from the narrower to the wider section of the capillary (initial  $\omega < 63^{\circ}$ ), the flow can be expected to stop at  $h_r = 14.8$  cm. For the same  $\omega$ , but with the flow proceeding from the opposite direction (initial  $\omega > 63^{\circ}$ ), the flow can be expected to stop at 14.6 cm. The true equilibrium position, which is not attained, is therefore between 14.6 and 14.8 cm. Although it cannot be expected to be exactly halfway between these two values, the most reasonable procedure is to use the intermediate value, here 14.7, as the likely equilibrium value of  $h_r$ . Any departure of the true-unattained-equilibrium position from this "halfway"  $h_r$  value is not large enough to be of consequence. This follows from the fact (Section VII) that results obtained on this basis yield  $\gamma$  values which agree with those reported in the literature. A further argument in favor of this "halfway" value will be given presently.

It is of interest in this connection to compare  $\gamma$  values calculated from the actually reached two limiting  $h_r$  values. Using the mean of such values given in Table I, one finds that the two values differ, on the average, by 1.03% and differ from their mean, on the average, by 0.51%-0.52%. The possible error committed on considering the "halfway" value and the equilibrium value of  $h_r$  as identical, is therefore very small ( $\ll 0.5\%$ ).

Figure 9 shows that the difference between the two final  $h_r$  values, reached on trying to approach equilibrium for a given  $\omega$  from opposite directions, is apparently independent of  $h_r$  excepting possibly very

TABLE I Surface Tension of Double Distilled Water at  $25.00^{\circ} \pm 0.05^{\circ}$ C. (Eq. [5] in conjunction with Eqs. [6a] and [7a])

Expt.	ω(°)	H(cm.)	$h_r(cm)$	$h_r - \frac{H}{2}$	$h_r + \frac{H}{2}$	$\gamma_i$	γ	
			1. Volume Us	ed: 1.667 × 1	$0^{-3} \ ml.$			
1a	60.10	2.2497	12.9898	11.8649	14.1146	72.79	72.53	
1b	59.82	2.1728	12.6163	11.5299	13.7027	72.26	12.00	
2a	61.26	2.5302	14.1062	12.8411	15.3713	73.25	72.93	
2b	61.26	2.4759	13.9057	12.6677	15.1436	72.60	14.90	
3a	61.63	2.5147	14.1110	12.8536	15.3683	72.05	71.88	
3b	61.68	2.4722	13.9155	12.6794	15.1516	71.71	11.00	
4a	61.68	2.5729	14.3194	13.0329	15.6058	73.11	72.13	
4b	61.85	2.4837	13.9243	12.6824	15.1661	71.14	12.10	
5a	63.00	2.7860	15.1795	13.7865	16.5725	72.83	72.68	
5b	62.73	2.7099	14.8881	13.5331	16.2430	72.53	12.00	
6a	63.90	2,9442	15.8348	14.3627	17.3069	72.21	71.80	
6b	64.28	3,0086	16.1525	14.6482	17.6568	71.39	11.80	
7a	64.00	2.9466	15.9955	14.5222	17.4688	72.17	72.04	
7b	64.28	2.9393	16.0412	14.5715	17.5108	71.90	72.09	
8a	64.46	3.0844	16.5312	14.9890	18.0734	72.40	71.95	
8b	64.45	3.0403	16.2951	14.7749	17.8152	71.49	71.90	
					Average:	$\overline{72.24}$		
		1	3. Volume Us	ed: 3.426 × 1	$0^{-8} \ ml.$		•	
9a	60.47	4.1501	13.0804	11.0053	15.1554	72.18	<b>5</b> 0.01	
9b	60.75	4.2338	13.2610	11.1441	15.3779	71.85	72.01	
10a	60.87	4.3158	13.4452	11.2873	15.6031	72.37	71 05	
10b	61.13	4.3205	13.4136	11.2533	15.5738	71.57	71.97	
11a	61.30	4.4768	13.8603	11.6219	16.0987	72.63	71 05	
11b	61.32	4.2395	13.7639	11.3209	16.2068	71.30	71.97	
					Average:	71.98		
				Overa	ll Average:	72.17		
		Deviation	n from literat			0.28%		

small drop volumes (curve pair III), for which points on the ascending and descending curve seem to differ less the wider the capillary section involved is. More systematic experiments are needed to clarify this point. The same applies to the question as to whether or not the drop volume has an effect on the difference between the ascending and the descending curve of a given pair of curves. This difference is practically the same for all volumes used  $(16.67-42.21 \times 10^{-4} \text{ ml.})$  except the smallest  $(11.06 \times 10^{-4} \text{ ml.})$ ; curve pair III).

It is worth while mentioning here that the difference of ascending and descending curves cannot be accounted for by minor drop evaporation, which would, of course, be a trivial effect. To con-

sider, for instance, curve pair II, the volume of the drop, as derived from H and  $h_r$ , was, near the beginning of this series,  $26.58 \times 10^{-4}$  ml. (average of volumes calculated for points 1 and 2). Nearly 8 hours later, the volume averaged for points 3 and 4 (points obtained near the conclusion of this series) was  $26.74 \times 10^{-4}$  ml. This difference is within the limits of experimental error.

It has been taken for granted thus far that the nonattainment of the true equilibrium position of the drop is due to surface roughness. No other reasonable explanation can be found. Moreover, the following considerations make this explanation also dynamically plausible: Considering again the  $h_r$  value of 14.7 at  $\omega = 63^{\circ}$  (curve pair II in Fig. 9), the pertinent  $R_1$  and  $R_2$  values

are  $1.295 \times 10^{-2}$  and  $1.557 \times 10^{-2}$  cm., respectively. Values of H and  $\alpha$  follow as 4.15 cm. and  $2 \times 10^{-6}$  steradian, respectively. From these data, one finds that for

TABLE II

COMPARISON OF PERFORMANCE OF RIGOROUS AND APPROXIMATING EQUATIONS USED IN CONNECTION WITH EQ. [5].  $\gamma_i$  VALUES (Using several experimental data of Table I)

Expt.	Eqs. [6],	Eqs. [6a], [7a]	Eqs. [6b],	Eqs. [43], [44]
3a	72.05	72.05	72.00	72.00
3b	71.70	71.71	71.65	71.65
8a	72.40	72.40	72.36	72.36
8b	71.49	71.49	71.45	71.45
9a	72.18	72.18	72.12	72.13
$^{9b}$	71.85	71.85	71.80	71.80
11a	72.63	72.63	72.58	72.59
11b	71.30	71.30	71.25	71.26

<sup>&</sup>lt;sup>a</sup> Equations in reference 1.

 $h_r = 14.7$  the excess surface pressure balanced by gravitational pressure would be 1870.4 dynes cm.<sup>-2</sup>. At  $h_r = 14.6$  and 14.8 the excess surface pressure would be 1861.8 and 1876.0 dynes cm.<sup>-2</sup>, respectively, and the gravitational pressure would be the same. The residual pressure which is unable to lead to a further movement of the drop towards its ideal equilibrium position is therefore 8.6 ( $h_r = 14.6$ ) and 5.6 dynes cm. $^{-2}$  ( $h_r = 14.8$  cm.), respectively. Expressed in millimeters of Hg, this is 6.4 ×  $10^{-3}$  and  $4.3 \times 10^{-3}$ , respectively. These figures show clearly that the dynamic differences between "ascending" and "descending"  $h_r$  vs.  $\omega$  curves are in fact so small that they may be accounted for by flow inhibition resulting from very minute irregu-

<sup>6</sup> The similarity of these residual pressures is a further argument in favor of the "halfway"  $h_r$  value as the most plausible equilibrium value.

TABLE III

Surface Tension of Aqueous NaCl Solutions at  $25.00^{\circ} \pm 0.05^{\circ}$ C. A: Outlining Recommended Detailed Procedure in Collection of Data

(Eq. [5] in conjunction with Eqs. [6a] and [7a]) (c: moles of NaCl per 1000 g. of solution)

Expt.	с	V <sup>25°</sup> C (ml. × 10 <sup>4</sup> )	ω <sub>a</sub> (degrees)	ω <sub>b</sub> (degrees)	$H_a$ (cm.)	$H_b$ (cm.)	$\gamma i_a$	$\gamma_{i}{}_{b}$	γ
1	0.5	24.63	60.87	60.93	3.4167	3.3435	73.37	72.48	72.93
$^2$	0.5	24.63	62.02	61.93	3.7065	3.6304	73.43	72.85	73.14
3	0.5	24.63	63.13	63.05	3.9811	3.8960	72.88	72.44	72.66
4	1.0	26.95	61.62	61.56	3.7699	3.6776	73.49	72.74	73.12
5	1.0	26.95	62.28	62.33	$3.9083$ $^{\circ}$	3.8718	73.35	72.82	73.09
6	1.0	26.95	63.80	63.66	4.4134	4.2946	73.27	72.81	73.04
7	1.5	27.12	60.70	60.59	3.6280	3.5137	75.56	74.62	75.09
8	1.5	27.12	61.78	61.93	3.8797	3.8678	75.61	75.08	75.34
9	1.5	27.12	62.23	60.28	4.0467	3.6181	75.33	74.29	74.81
10	1.5	27.12	63.57	63.50	4.3802	4.3802	74.73	74.36	74.55
11	2.0	29.06	60.33	60.31	3.6688	3.5904	75.67	75.08	75.38
12	2.0	29.06	60.93	61.01	3.9224	3.8294	75.87	75.17	75.52
13	2.0	29.06	62.77	63.26	4.4557	4.4990	76.08	74.75	75.42
14	2.5	23.62	61.15	61.15	3.1593	3.0378	76.90	75.89	76.39
15	2.5	23.62	62.15	62.14	3.3272	3.3051	76.38	75.98	76.18
16	2.5	23.62	63.32	63.26	3.6336	3.5305	76.43	75.43	75.93
17	2.5	23.62	63.73	63.66	3.7161	3.5250	76.25	74.65	75.45
18	3.0	25.84	63.20	63.10	3.9570	3.7815	77.83	76.40	77.12
19	3.0	25.84	64.41	64.32	4.3149	4.1515	77.20	76.12	76.66
20	3.5	23.31	59.95	60.02	2.7568	2.6019	78.38	76.89	77.64
21	3.5	23.31	61.71	61.67	3.1871	3.0695	78.41	77.00	77.70
22	3.5	23.31	62.00	61.78	3.2445	3.0596	78.29	76.76	77.53
23	3.5	23.31	63.55	63.48	3.6233	3.4568	78.06	76.46	77.26
24	4.0	25.71	63.21	63.40	3.9174	3.7656	79.52	77.40	78.46
25	4.0	25.71	64.00	62.21	4.1079	3.3088	78.90	78.42	78.66
26	4.0	25.71	64.69	64.92	4.4052	4.2590	79.05	77.21	78.13

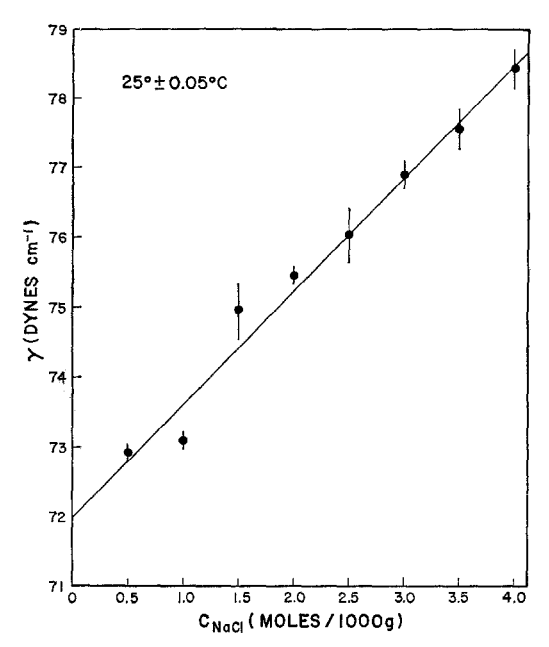


Fig. 10. Surface tension of aqueous NaCl solution as a function of molality.

larities of the capillary surface (surface roughness).

In conclusion, it may be mentioned that the preliminary results illustrated by Fig. 9 may possibly open the door for a quantitative determination of surface roughness of inner capillary walls.

#### VII. RESULTS

## 1. The Surface Tension of Distilled Water

Table I gives the results obtained for two drops of double distilled water one having a volume of  $16.67 \times 10^{-4}$ , the other one of  $34.26 \times 10^{-4}$  ml. Experiments defined by numbers followed by "a" refer to the final position of the conical drop of water after flowing from the smaller towards the larger

end of the capillary; experiments identified by numbers followed by the letter "b" pertain to the inverse direction of flow. Each of these pairs of measurements differs from the others in the average  $\omega$  value. The individual  $\omega$  values within a pair (2nd column) were made as similar as practically possible without lengthy trials. The over-all variation of  $\omega$  was 4.6°, which led to a change in  $h_r$  by 3.9 cm. The extreme positions of the menisci-defined by  $[h_r - (H/2)]$  and  $[h_r +$ (H/2), respectively—were reached in experiments 9a and 8a, respectively, and are indicated by the arrows in Fig. 5. The entire range of the capillary utilized was therefore 7 cm., i.e., a little more than half the useful calibrated section of the capillary. It is defined by a minimum and maximum capillary radius of 0.124 and 0.171 mm., respectively.

The individual  $\gamma$  values,  $\gamma_i$ , refer to a single measurement. They are, as stated, affected by surface roughness. The significant  $\gamma$  values given in the subsequent column are those obtained on averaging the results of one pair of measurements. These  $\gamma$  values do not show any systematic variation with  $\omega$  or  $h_i$ , nor can one detect any systematic variation of  $\gamma$  with the volume of water used. The largest and smallest of the eleven  $\gamma$  values obtained (72.93 and 71.80 dynes cm.<sup>-1</sup>) differ by -0.2% and 1.3% from the literature value of 71.97. The mean of the eleven  $\gamma$  values (72.17) differs from the literature value by only 0.28%. These results are a very gratifying proof of the high accuracy of absolute  $\gamma$  values obtainable with the microcone tensiometer. Even more accurate  $\gamma$  values can be expected with capillaries of constant  $\alpha$ , where uncertainties in calibrations would be eliminated almost completely.

TABLE IV Surface Tension of Aqueous NaCl Solutions at  $25.00^{\circ}\pm0.05^{\circ}\mathrm{C}$ . B: Final results and comparison with literature data.

c	0.5	1.0	1.5	2.0	2.5	3.0	3.5	4.0
$\gamma_{av}$ .	72.91	73.08	74.95	75.44	76.02	76.89	77.55	78.43
	$\pm 0.2$	$\pm 0.1$	$\pm 0.4$	$\pm 0.1$	$\pm 0.4$	$\pm 0.2$	$\pm 0.3$	$\pm 0.3$
$\gamma_L$	72.78	73.59	74.40	75.24	76.04	76.86	77.67	78.50
	$\pm 0.1$	$\pm 0.1$	$\pm 0.1$	$\pm 0.1$	$\pm 0.2$	$\pm 0.2$	$\pm 0.2$	$\pm 0.2$
$\Delta(\%)$	+0.17	-0.71	+0.74	+0.27	-0.03	+0.04	-0.15	-0.10

The results given in Table I were obtained with Eq. [5] in conjunction with the simple equations [6a] and [7a]. Table II shows for 8 of the  $22\gamma_i$  values the results on using, in addition, other equations. The first pertinent column shows the results obtained with the rigorous equations [6] and [7]. It is seen that the results obtained with the simplified equations [6a] and [7a] used in Table I and repeated in column 2 are quantitatively the same. This could be expected for water  $(\beta = 0)$  and the small  $\alpha$  value of the capil-

TABLE V
INSTRUMENT CONSTANT, C, FOR THE  $h_{\tau}$  RANGE 11.50-16.00 Assuming Use of Calibration Curve II in Fig. 4
Literature value of  $\gamma$  used: 71.97 dynes cm.<sup>-1</sup>.

Expt.*	$\gamma_{ap}$ .	$D \times 10^4 \ (cm)$
1a	74.75	2.49
1b	74.09	2.49
2a	75.47	2.35
2b	74.60	∠.59
3a	74.44	2.35
3b	73.81	2.00
4a	74.41	2.34
4b	73.52	2.04
Avera	ige: $\overline{74.39}$	
	$C: 3.253 \times 10$	-2
	$\bar{D}$ : 2.38 × 10 <sup>-1</sup>	4

<sup>\*</sup> The numbers in this column refer to the respective experiments in Table I.

lary used. The results obtained with the still simpler equation [6b], differ, as fore-seen, in the fourth figure. Finally, results are given on using equations which differ from those given here in the treatment of the gravitational (hydrostatic) pressure but which incorporate approximations identical with those contained in Eqs. [6a] and [7a].

## 2. The Surface Tension of NaCl Solutions

### A. Absolute $\gamma$ Values.

Table III gives the results on the variation of  $\gamma$  with the concentration of aqueous NaCl solutions. The letter a, used here as a subscript to  $\gamma_i$  identifies again the results obtained on flow from the narrow to the wide end of capillary; the subscript b refers to the inverse direction of flow prior to establishment of the final drop position. At least two such pairs and at the most four pairs of measurements were made with each drop. The individual  $\gamma_i$  values obtained for each pair,  $\gamma_{ia}$  and  $\gamma_{ib}$ , were averaged to yield  $\gamma$ . The averages,  $\gamma_{av}$ , of these 2-4  $\gamma$  values are compared in Table IV with the literature values,  $\gamma_L$  (2). They differ from them at the most by 0.7% and, on the average, by 0.3%. Figure 10 illustrates the results. The straight line represents the mean of the literature data. The full circles are the  $\gamma_{av}$  values as given in Table IV and

TABLE VI Surface Tension of Aqueous NaCl Solutions Calculated by Means of Calibration Curve II in Fig. 4 and the Instrument Constant C Given in Table V

Expt.	NaCl (moles/1000 g.	$h_r - \frac{H}{2} (cm.)$	$h_r + \frac{H}{2}$ (cm.)	H (cm.)	$(\gamma_i)_{ap}$ .	$(\gamma_{ap.})_{av.}$	$\gamma_c$	$\gamma L$	Δ(%)
1a	0.5	11.6620	15.0789	3.4167	74.55				
1b	0.5	11.4655	14.8090	3.3435	74.21				
						74.55	72.12	72.78	-0.91
2a	0.5	12.4052	16.1117	3.7065	75.12				
2b	0.5	12.1961	15.8265	3.6304	74.31				
8a	1.5	11.8045	15.6842	3.8797	76.90				
						76.63	74.14	74.40	-0.35
8b	1.5	11.7623	15.6304	3.8678	76.36				
15a	2.5	11.8530	15.1802	3.3272	78.36				
						78.23	75.69	76.04	-0.46
15b	2.5	11.7676	15.0727	3.3051	78.10				
21a	3.5	11.5689	14.7560	3.1871	80.09				
	3.0	: 0000				79.49	76.90	77.67	-0.99
21b	3.5	11.2431	14.3126	3.0695	78.88				

the length of the bars represents the maximum spread of the individual  $\gamma$  values in Table III.

### B. $\gamma$ Values Obtained by Means of an Instrument Constant

If one does not aim for the highest possible accuracy of the  $\gamma$  values, one may simplify the calibration procedure and convert relative  $\gamma$  values into absolute  $\gamma$  values by means of an instrument constant, C. The practical usefulness of this possibility, outlined in Section IV, was tested on the NaCl solutions. Since a single constant C can apply only to a limited section of the capillary, this section had to be picked. For the sake of convenience, the section encompassed by Fig. 4  $(h_r: 11.5-16.0 \text{ cm.})$  was selected. Eight of the twenty-two experiments, with water, considered in Table I pertain to conical drops the entire length of which was within these limits. On the assumption that only the calibration curve II of Fig. 4 is available (obtained with 40.1 mg. Hg), the apparent  $\gamma$  values,  $\gamma_{ap}$ , given in Table V are obtained for these eight experiments. These  $\gamma_{ap}$  values are, of course, far too high. From their average, 74.39, and the literature value, 71.97, the instrument constant C is obtained at once by means of Eq. [24]. In addition, the individual D values, resulting from Eq. [25], and their mean,  $\bar{D}$ , are calculated.

Table VI gives the individual apparent  $\gamma$  values  $(\gamma_i)_{ap}$  obtained for several of the NaCl solutions considered in Table III using calibration curve II of Fig. 4. Experiments are excluded in which  $(h_r + H/2)$  and  $(h_r - H/2)$  were appreciably outside of the range of  $h_r$  values for which C was obtained in Table V. From these individual apparent  $\gamma$  values, the average apparent  $\gamma$  values,  $(\gamma_{ap})_{av}$  are obtained. If we now use

the instrument constant, the corrected  $\gamma$  value,  $\gamma_c$ , is obtained. The last column gives the per cent deviation of  $\gamma_c$  from the literature value  $\gamma_L$  repeated in the preceding column. The  $\gamma_c$  values are clearly less good than those obtained on operating the method as an absolute method (Table IV). For some purposes, however, the error of 0.4%-1.0% will not be considered serious enough to forego the convenience of the relative  $\gamma$  determinations by means of an instrument constant.

#### SUMMARY

A brief survey is given on the theory of a new method for determining the surface tension of very small amounts of liquids or solutions  $(10^{-3}-10^{-4} \text{ ml.})$ . The method is based on the fact that a liquid drop in a conical capillary will, in the absence of compensating factors, flow towards the tip owing to an imbalance of surface pressures at the two menisci. This imbalance can be relieved by proper inclination of the capillary, i.e., by proper hydrostatic pressure. A simple apparatus is described by means of which surface tensions of water and of aqueous NaCl solutions were determined with an average error not in excess of 0.3%. A detailed description of the rather elaborate calibration technique is given which is needed if the method is to give absolute surface tensions. An alternate much simpler, but less accurate, principle is also discussed which involves the use of an instrument constant. The relatively small but pronounced effect of surface roughness and a simple method for eliminating its effect from the results is also discussed.

#### REFERENCES

- Heller, W., J. Chem. Phys. 40, 3292 (1964).
- International Critical Tables, Vol. IV. Mc-Graw-Hill, New York, 1928.